which upon substituting in the respective equations will yield R from field data. Some resultant maximum potentials are: (after Telford and Alex Becker, 1965) graphite 780 mV, pyrite (FeS) 730 mV, galena (Pbs) 330 mV, etc.

Another aspect of the experimentation was establishing the relationship between the current I and the surface area of the ore body in contact with the electrolyte. This was found as linear (of the form $y = mx + c$) in Figure 2 through working on a Daniel cell-type setup (Figure 1), with an orebody (iron or zinc rod in the experiments) taken in a porous pot containing aqueous solution of dilute H_2So_4 as one electrode which is placed in the electrolyte in a copper vessel. The copper vessel acts as the other electrode. Variation of depth of immersion of the iron or zinc rod in the porous pot or changing the depth of immersion of the porous pot in the copper vessel causes a variation in the current strength being recorded in the circuit. Now in equation (3) if ρ value is substituted and I is obtained after conventional stages of interpretation, the graph (Figure 2) between I and the surface area of the electrode in contact with the electrolyte can be used to read the area of the orebody lying in the zone of saturation. Doubling this value will yield the total surface area of the orebody and therefore from 2a value the thickness of the sheet can be determined.

Further experiments towards standardizing the relationships are in progress.

Limitations

(1) Naturally occurring orebodies may not confine to simple regular geometric models. (2) The range of variation of electrical properties is very wide and therefore large deviations of the interpreted sizes from the actual are likely. Nevertheless, in the absence of any established techniques for quantitative size determination of SP sources, the presently suggested approach could be reasonably used and with the advanced level of electronic measuring systems, standardizing the values of I and ρ is quite possible.

Reference

Becker, Alex, and Telford, W. M., 1965, Spontaneous polarization studies: Geophys. Prosp., 13, 173–188.

Airborne Electromagnetic Bathymetry EM3.7

A. Becker, H. F. Morrison, R. Zollinger, Univ. of California, Berkeley; and P. G. Lazenby, Questor Surveys Ltd., Canada

A specialized automated simple inversion technique was developed for the interpretation of airborne time-domain electromagnetic (TDEM) offshore data obtained in coastal areas. This method was tested on a limited amount of data that was acquired in Canada with the Barringer/Questor MKVI Input® airborne TDEM system along a 17 mile long flight path off the coast of Cape Breton Island in the Province of Nova Scotia. A preliminary analysis of the data and comparison of the results with the available bathymetric charts indicates that the data can be interpreted to an accuracy of the order of ±1.5 m in areas where the depth of sea water does not exceed 20 m.

Introduction

Traditionally, airborne electromagnetic (AEM) systems have been used for the detection of distinct, anomalous subsurface conductors. As equipment quality improved, however, all of the state-of-the-art apparatus can now be also employed for mapping ground conductivity. Thus Dyck et al. (1974), Whiting (1983), and most recently DeMoully and Becker (1984) reported the use of the towed bird time-domain Input system for mapping the conductivity and thickness of surficial materials. Similar applications of frequency apparatus were reported by Fraser (1978) for the Dighem helicopter system and by Seigel and Pitcher (1978) for the fixed wing Tridem system. The Input results reported in the references cited above are of particular relevance to this paper since they clearly demonstrate the accurate airborne measurement of thickness and conductivity of a highly conductive surficial layer. Evidently, the data interpretation techniques used for geological interpretation can be readily adapted for purposes of airborne bathymetry. Indeed, the feasibility of using a conventional AEM system for bathymetry was confirmed by Morrison and Becker (1982) in a report submitted to ONR. Their analysis of conventional survey systems shows that the Input system appears to be particularly well suited for the task. It can resolve a 40 m depth to better than 3 percent and a 60 m depth to about 15 percent.

In parallel with improvements in data quality, the last decade also witnessed the evolution of appropriate theoretical methods for data analysis. Because of the amount of data that needs to be interpreted, it is impractical to use classical inversion techniques (c.f., Glenn et al., 1973) for the analysis of time-domain AEM data. Instead, as shown in the literature cited, the field data can be best interpreted using automated, noninteractive, nomogram fitting techniques based on the assumption of very simple geologic models.

Survey parameters

The survey data were acquired with the towed bird, time-domain Barringer/Questor Mark VI Input system in its standard (horizontal axis receiver positioned 100 m behind and 70 m below the aircraft) configuration. A two ms pulse was used to induce transient eddy currents in the sea water.

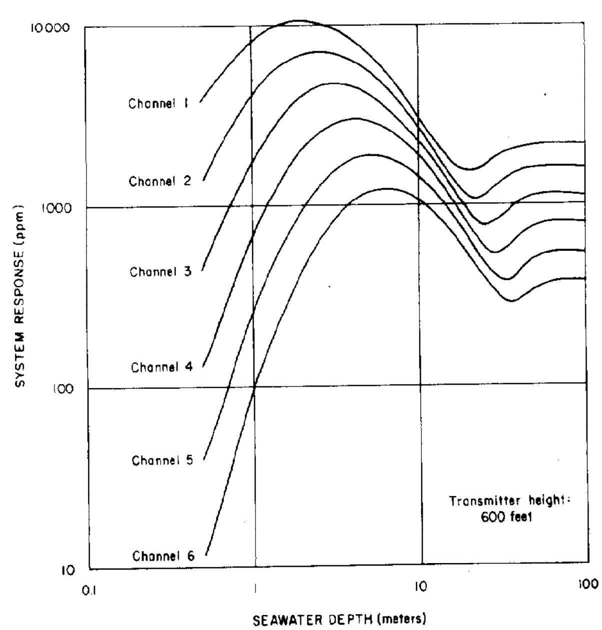

Fig. 1. Conventional Palacky INPUT response diagram for variable water depth. Seawater conductivity taken as 1 s/m.

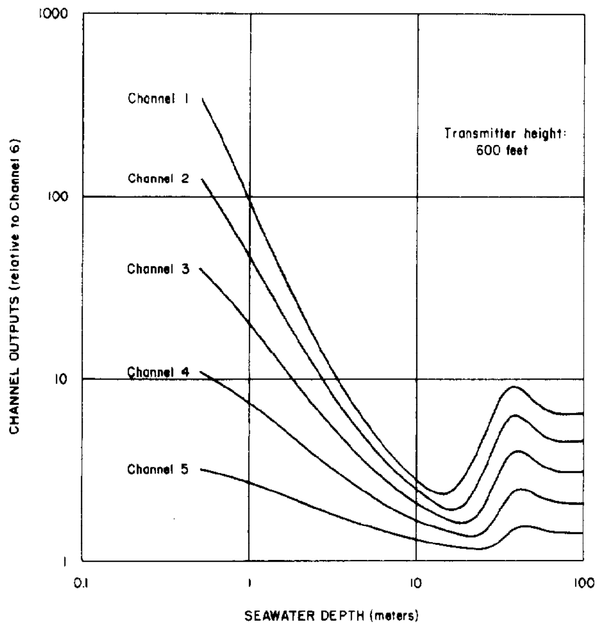

FIG. 2. Relative INPUT response for variable water depth.

The decay of the secondary magnetic fields was measured with a conventional 6-channel detector.

The test survey was done by Questor Surveys Ltd. of Toronto, in conjunction with a mineral survey near Cape Breton Island in the Canadian Province of Nova Scotia. All the data relate to a single 17 mile long flight line which is oriented roughly east-west and crosses the mouth of the Lennox Passage. The center of the line is located at 45°35'N, 60°50'W. Detailed bathymetry for this area is available as shown on two Canadian Coastal charts for St. Peters Bay. (no. 4275, 1:30,000; and no. 4308, 1:37,500). The survey line was repetitively flown six times. The data were acquired at altitudes of 600, 700, and 800 ft in both the east and west directions. In addition to the analog records, the flight data, including altimeter and magnetometer values are also recorded in digital form on computer-compatible magnetic tapes. Thus it is readily accessible for automated interpretation on a high speed digital computer. On survey, the aircraft maintains a speed of about 120 mph or 175 ft/s. The detector output is scanned twice a second so that the data interval corresponds to a linear distance of about 90 ft.

Data interpretation

In interpreting offshore AEM data it is reasonable to assume a single layer model made up of the conductive sea water overlying a very resistive half-space of bottom sediments and basement rocks. The problem is further simplified by considering the conductivity of sea water to be constant at 4.0 S/m, and by assuming that the bottom is infinitely resistive. The only unknown parameter then, is the depth of sea water. It may be determined by comparing the observed electromagnetic transients to a table of theoretical values computed for various depths of sea water.

Figure 1 shows theoretical data values for the simple

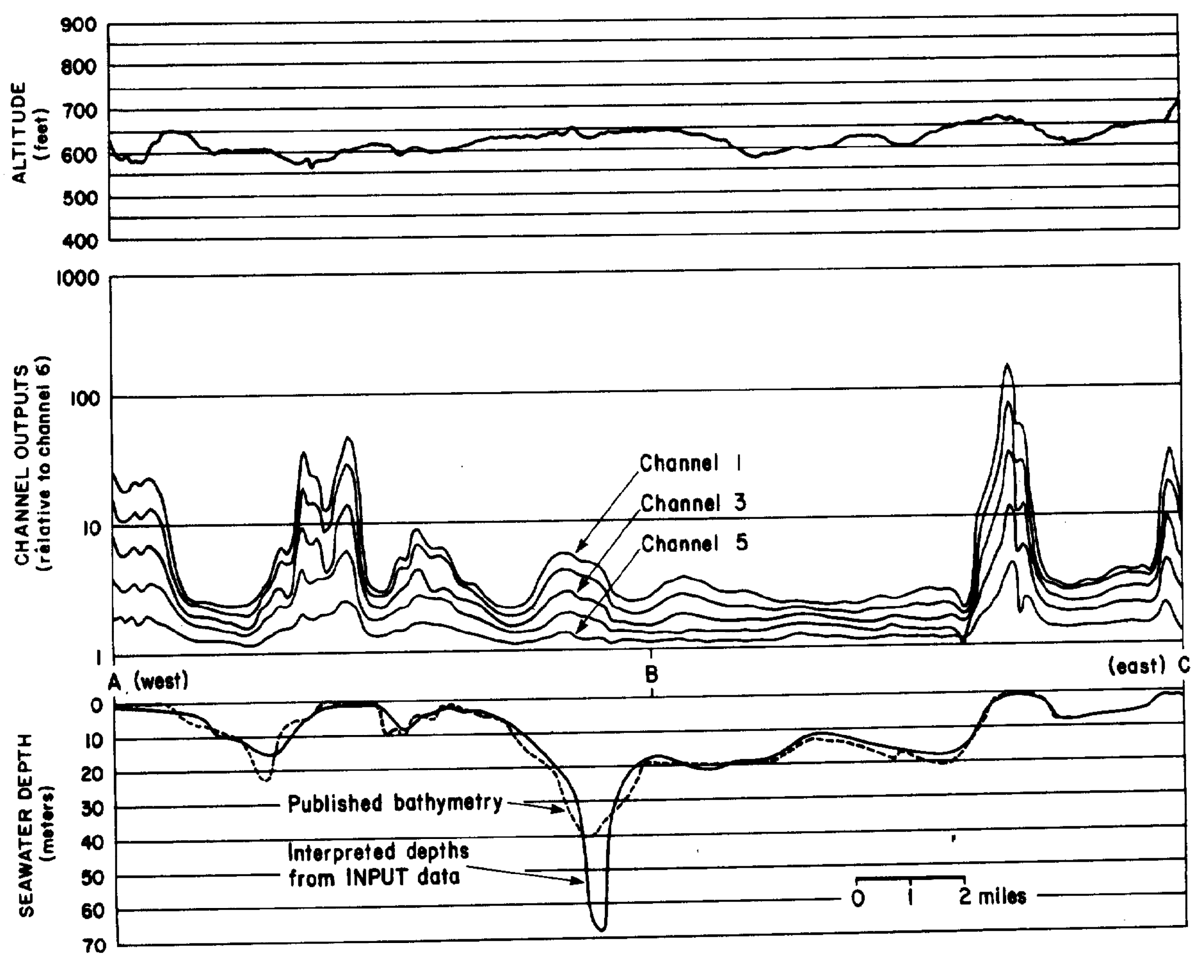

FIG. 3. Normalized INPUT data and interpreted bathymetry.

model described above. The presentation is done in the form of a conventional Palacky diagram which illustrates the variation of system response as a function of sea water depth. The theoretical data show excellent depth resolution for this system, out to depths of about 20 m and fair resolution out to depths of about 50 m. Beyond that depth, the sea water layer resembles a conductive half-space.

In areas of very high surficial conductivity, the amplitude of the secondary field transient is a very sensitive fraction of system elevation and geometry. While the transient shape is relatively insensitive to these effects, it is mainly related to the thickness and conductivity of the surficial layer. Thus an optimal data interpretation technique for this problem should rely on the relative channel amplitudes rather than on their absolute values. Figure 2 shows the data of Figure 1 replotted in this form. All channel amplitudes have been normalized by the amplitude of the sixth channel in order to remove the effects of system geometry on the absolute amplitude of the response without distorting the transient shapes. The results in Figure 2 were computed for a transmitter height of 600 ft above sea level but similar data were generated for all other transmitter heights at 50 ft intervals in the range of interest.

Experimental results

Normalized data for one traverse of the 17 mile long flight line is shown in the upper part of Figure 3. The altimeter record is shown above the electromagnetic field data. The depth of sea water along this line may be found immediately by comparing the normalized amplitudes of channels 1–5 with the theoretical curves in Figure 2. These data are one of six sets collected by Questor Surveys while flying this line repetitively, east and west, at 600, 700 and 800 ft above sea level. Each of these records was inverted individually. The six depth profiles were then combined to obtain the final interpreted depth profile shown in the lower part of Figure 3. The corresponding published bathymetry from Canadian Coastal Charts of St. Peter's Bay (4275 and 4308) is also plotted for comparison with the interpreted data. The agreement between the interpreted AEM depths and the published bathymetry is quite good, generally agreeing within 2 m when the water is less than 20 m deep. As anticipated, the short wavelength variations in the survey data that relate to amplitude changes were removed from the interpreted section by the normalizing procedure. The single major discrepancy between the interpreted section and the conventional bathymetry occurs near point B where we traversed the Lennox Passage. This relatively narrow feature is probably filled with saturated unconsolidated sediments which from an electrical point of view cannot be distinguished from sea water. It is also possible that the depths in the Lennox Passage at this point are not accurately charted.

Conclusions

By using a simple one-layer model and an efficient table look-up scheme, large volumes of offshore AEM data may be interpreted accurately and inexpensively in terms of sea water depth. This technique could make AEM surveys a viable alternative to present methods for obtaining bathymetric data. Although the accuracy of airborne electromagnetic bathymetry is limited in deep waters by the "skin depth" at the pulse repetition frequency this new method of obtaining bathymetric data appears to be very useful in shallow coastal waters.

References

DeMoully, G. T., and Becker, A., 1984, Automated interpretation of airborne electromagnetic data: Geophysics, **49**, 400–407.
Dyck, A. F., Becker, A., and Collett, L. S., 1974, Surficial conductivity mapping with the airborne INPUT system: CIMM Bull., **66**, 104–109.
Fraser, D. C., 1978, Resistivity mapping with an airborne multicoil electromagnetic system: Geophysics, **43**, 142–172.
Glenn, W. E., Ryu, J., Ward, S. H., People, W. J., and Phillips, R. J., 1973, The inversion of vertical magnetic dipole sounding data, Geophysics, **38**, 1109–1129.
Morrison, H. F., and Becker A., 1982, Analysis of airborne electromagnetic systems for mapping depth of sea water: Final rep., ONR, contract N00014-82-M-0073, 1–57.
Seigel, H. O., and Pitcher, D. H., 1978, Mapping earth conductivities using a multifrequency airborne electromagnetic system: Geophysics, **43**, 563–575.
Whiting, T. H., 1983, Surficial conductivity mapping with INPUT airborne EM system and its application to coal exploration: Proc. 4th Int. Coal Symp., Sydney, Australia, 17 pp.

The Response of the Elrec Sonde to a Salt Dome or a Regional Dip EM3.8

R. Chemali, S. Gianzero, Gearhart Industries Inc.; and A. Nekut, Amoco Production

Previous publications on the Elrec logging tool have only emphasized its ability to locate a remote casing. The present paper demonstrates that it is feasible to use an Elrec tool both to define the position of a salt dome and to determine the azimuth and magnitude of a regional dip. The Elrec sonde measures the magnetic field induced by a current source in a crossed pair of magnetometers located below the source. In the simple situation where the geologic beds exhibit an axisymmetrical resistivity pattern about the sonde and the wireline, the net measured magnetic field is identically zero.

The presence of a conductive or resistive anomaly or a regional dip perturbs the axial symmetry of the current and induces a measurable field in the magnetometers. A massive resistive anomaly is modeled as a planar interface or a spherical shape (i.e., salt dome). An exact formula is given for either case, and a series of simulated logs is shown for various sizes of spherical anomalies. The regional dip is modeled by computing the response of the Elrec in an anisotropic formation such as a laminated shale. The model is then expanded to include a thin dipping bed. The applicability of Elrec to determine the regional dip is illustrated in an actual log example.

In addition, a complete analysis for the detection of casing, including an anisotropic formation, is developed and incorporated into an interactive program for use at the well site.

Introduction

The Elrec logging tool was originally conceived and developed as a sensor capable of locating a remote casing experiencing a blowout. It has the unique capability of indicating both the direction and distance to the target, with a range of investigation of a few hundred feet. Publications to date (West et al., 1983; Kuckes et al., 1981, 1984) only addressed the specific application of locating a remote casing. In the present paper we evaluate, through mathematical modeling,